

Castor Oil and Sorbitan Monopalmitate Based Organogel as a Probable Matrix for Controlled Drug Delivery

Vinay K. Singh,¹ Kunal Pal,¹ Dillip K. Pradhan,² Krishna Pramanik¹

¹Department of Biotechnology and Medical Engineering, National Institute of Technology, Rourkela 769008, India

²Department of Physics, National Institute of Technology, Rourkela, 769008, India

Correspondence to: K. Pal (E-mail: pal.kunal@yahoo.com)

ABSTRACT: The study has been designed to develop and evaluate the *in vitro* sustained-release capability of sorbitan monopalmitate (SMP) and castor oil (CO) based organogels. Organogels were prepared by heating the mixture of SMP-CO at 60°C either with or without using distilled water (DW). The heated mixture was subsequently cooled to room-temperature to allow the formation of a gelled structure. Characterization of organogels was carried out by microscopy (light, fluorescent, electron, and atomic force), Fourier transform infrared (FTIR) spectroscopy, X-ray diffraction (XRD), differential scanning calorimetry (DSC), rheological study, pH, impedance spectroscopy, hemocompatibility, and antimicrobial studies. The properties and stability of the gels was dependent on the composition of the organogels. FTIR studies indicated the presence of strong intramolecular/intermolecular hydrogen bonding amongst the gel components. XRD studies suggested amorphous behavior of the gels. The gels showed a shear thinning behavior. Metronidazole (MZ) loaded gels showed good antimicrobial property to be used as an antimicrobial formulation. © 2013 Wiley Periodicals, Inc. *J. Appl. Polym. Sci.* 130: 1503–1515, 2013

KEYWORDS: drug delivery systems; gels; kinetics; microscopy

Received 8 November 2012; accepted 25 February 2013; Published online 30 April 2013

DOI: 10.1002/app.39315

INTRODUCTION

Semisolids formulations have often been used to develop topical body products (e.g., ointments, creams, gels, suppositories, pastes, and pessaries), which when applied to the skin or mucous membranes tend to improve or treat pathological conditions and/or offer protection against injuries.^{1,2} Gels have been defined as semi-solid formulations/products which are composed of gelator molecules (usually having concentration <15%) and a solvent phase. The gelators may self-assemble, either by physical or chemical interactions, to form a mesh network. The network helps immobilizing the solvent phase and do not allow the flow of the solvent out of the network. This has been attributed to the surface active phenomena amongst the gelator network and the solvent.^{3–6} The composition of the gels may be tailored to contain drugs (e.g., ciprofloxacin and metronidazole), solvents (e.g., alcohol, propylene glycol, sunflower oil, mustard oil, and soybean oil), preservatives (e.g., methyl paraben, propyl paraben, and chlorhexidine gluconate) and/or stabilizers (e.g., edetate disodium).^{7–11} Depending on the composition of the gels, the physical and chemical interactions among the gel components may vary and hence their

physicochemical properties.^{12,13} The gels may be categorized either as hydrogel or organogel. Hydrogels may be defined as semi-solid formulation which contains polar solvent. On the other hand, organogel contain apolar solvent within its 3D structure.¹⁴ The organogels may further be categorized either as fluid-filled fiber matrix and solid-fiber matrix organogels.¹⁵ With the advancements in the pharmaceutical, food, nutraceutical, and cosmetics industries, various organogel-based products are being developed for human consumption.^{3,16}

Sorbitan monopalmitate (SMP), an ester of sorbitan (a sorbitol derivative) and stearic acid, has often been referred to as a synthetic wax. It is commonly used as an emulsifier to formulate emulsions.¹⁷ It is a non-ionic surfactant composed of natural fatty acid (palmitic acid) and the sugar alcohol (sorbitol) within its chemical structure. SMP forms a film at the interface of the oil and water thereby reducing the interfacial tension amongst the emulsion components. SMP have been used extensively as a surfactant to develop various pharmaceutical and cosmetic products.^{9,18–20}

Castor oil (CO) is an unsaturated fatty acid (rich in ricinoleic acid) extracted from the seeds of castor plant (*Ricinus communis*).²¹

Additional Supporting Information may be found in the online version of this article.

© 2013 Wiley Periodicals, Inc.

It is pale yellow in color and exhibits anti-inflammatory and anti-oxidant properties.²² It has been used since long in the formulation of various pharmaceutical products (e.g., contraceptive creams, synthetic flower scents, formulation of bland emollient for curing skin disease, and for inducing labor in pregnancy).^{23–25} CO-based derivatives have been used to develop synthetic detergents with antimicrobial properties.²

In this study, attempts were made to develop and characterize CO-based organogels, using SMP as the organogelator, for probable applications in controlled drug delivery. Metronidazole (MZ) was used as a model drug. The release kinetics of the drug from the CO-based organogels has been studied in details. Further attempts were also made to analyze the antimicrobial properties of the gels.

MATERIALS AND METHODS

Materials

SMP and MZ were purchased from Loba Chemie Pvt., Mumbai, India and Aarti drugs, Mumbai, India, respectively. Nutrient agar and dialysis tubing (MW cutoff: 60 kDa) were purchased from Himedia, Mumbai, India. Microbial cultures of *Bacillus subtilis* (NCIM 2699) and *Escherichia coli* (NCIM 2563) were obtained from NCIM, Pune, India. CO was purchased from Loba Chemie Pvt., Mumbai, India. Double distilled water (DW) was used for all experimental studies.

Methods

Preparation of Organogel. Accurately weighed SMP was dissolved in CO, kept on stirring at 60°C at 500 rpm to form a hot solution of SMP in CO. The hot solution, so formed, was transparent. The solution was cooled down to the room-temperature (RT). As the temperature was reduced, the transparent solution formed a turbid suspension. The turbid suspension, upon further standing, either remained as a suspension or formed a stable gel. The concentration of SMP was varied from 1% (w/w) to 30% (w/w) to figure out the critical gelator concentration (CGC).²⁶ The gel sample at CGC was regarded as G. The samples were regarded as organogel, if the sample failed to flow on inversion of vial.^{27,28}

The property of the G gel was modulated by incorporating water into the gel structure. The method of preparation of water-containing gels was similar to the method described above. In short, specified amount of DW, maintained at 60°C, was added to the hot solution of SMP in CO, kept on stirring at 60°C at 500 rpm. The rest of the procedure was same. Depending on the proportions of the SMP–GNO–DW mixture, a gel formulation or an emulsion was obtained upon cooling the mixture to RT.²⁹ The gels containing water was regarded as GW.

MZ, a model antimicrobial drug, was incorporated to the gels so as to have a drug concentration of 1% (w/w) in the formulation. The drug was dispersed in the hot solution of SMP in CO. The dispersion was used for the preparation of the organogel.³⁰

Organoleptic Evaluation. Organogels were evaluated for their color, odor, texture, appearance, and taste.³¹

Accelerated Stability Test. Freshly prepared organogels were subjected to alternate freeze–thaw (FT) cycles. Each cycle of

freeze–thaw consisted of 15 min of cooling at $-5 \pm 1^\circ\text{C}$ and 15 min of thawing at $70 \pm 1^\circ\text{C}$. The experiment was continued for five cycles. The gel samples were analyzed for any destabilization at regular intervals. The effect of thermocycling on the structural integrity of the gels was also studied by microscopic study. A sample may be regarded as stable if it can withstand for at least five cycles of thermocycling.¹⁶

Long-Term Stability Study. The gels found to be stable under accelerated conditions, were subjected to long-term stability test. The gels were incubated at $25 \pm 2^\circ\text{C}$ and 60% RH $\pm 5\%$ RH for 12 months as per the ICH guidelines. The color or consistency of the product was checked at regular intervals of time for any signs of destabilization.³²

Microscopic Studies. The microstructures of the gels were studied by optical microscopy (OM), fluorescence microscopy (FM) and scanning electron microscopy (SEM), and atomic force microscopy (AFM).

An upright optical microscope, Lieca DM 750 equipped with ICC50HD camera was used to analyze microstructure of the organogels. The mechanism of the organogel formation of the gels was studied.³³ The droplet size diameters of the dispersed phase of water containing gel samples were determined using NI Vision Assistant-2010 as per the reported literature.³⁰

The xerogels of both G and GW were analyzed under scanning electron microscope (SEM) (Jeol JSM-6480LV, Japan). The xerogels were prepared as per the method reported elsewhere.⁹ The xerogels were sputter-coated with platinum before analysis.

FTIR Spectroscopy. The raw materials and the gels were analyzed using AlphaE ATR-FTIR, Bruker. The samples were analyzed in the range $500\text{--}4000\text{ cm}^{-1}$. The instrument was working in the attenuated total reflectance (ATR) mode.³⁴

X-ray Diffraction Study. The position, intensity, width, and shape of diffraction peaks of the gels were studied by X-ray Diffraction (XRD) to have an understanding on the crystallinity of the formulations.³⁵ SMP, MZ, CO, blank gels, and gels loaded with MZ were subjected to XRD analysis using Philips, XRD-PW 1700, Rockville. Monochromatized Cu $K\alpha$ was used as the X-ray source and was operating at 30 kV. The current flow in the tube was at 20 mA. Samples were scanned in the diffraction angle range of $5\text{--}50^\circ 2\theta$ at a scan rate of $2^\circ 2\theta$ per min.³⁶

Impedance Spectroscopy. The electrical behavior of the gels was studied using a computer-controlled impedance analyzer (NEWTONS 4th LTD: PSM 1735, UK). An ac voltage of 100 mV was applied across the copper electrodes. Complex impedance parameters (e.g., impedance, dielectric permittivity, and tangent loss parameters) were studied in the frequency range of 0.1 Hz to 1 MHz at RT. The ac conductivity (σ_{ac}) was evaluated from the dielectric measurements.³⁷ The real (Z') and imaginary (Z'') parts of impedance were calculated.³⁸

Viscosity Analysis. Viscosity measurements of the freshly prepared gels were carried out at a controlled temperature of $25 \pm 0.1^\circ\text{C}$ using a cone-and-plate viscometer (Bohlin visco 88, Malvern, UK). The cone was having a cone angle of 5.4° and a diameter 30 mm. The gap between the cone and the plate was

set at 0.15 mm. The induced response (strain) was measured when a sinusoidal stress was applied to the gels. The viscosity (η) and stress (σ) of the sample were obtained from the steady-shear measurement when the shear rate was varied from 10–100 s^{-1} and 100–10 s^{-1} using steady-state flow model.³⁹

Texture Analysis. The mechanical behaviors (e.g., stress relaxation and spreadability) of the developed gels was studied by TAHD Plus Texture Analyzer (Stable Microsystems, TA-HDplus, UK). The tests were conducted using a 45° perspex cone. The samples were kept in a matching female cone. The stress relaxation test was carried out by penetrating the conical probe up to a target distance of 5 mm (after a trigger force of 3 g) at a rate of 0.5 mm/s to induce a stress in the samples. The probe was held at the target distance for a period of 30 s and the corresponding changes in the stress were recorded.^{40,41} The spreadability of the samples was also carried out in the same fixture. The male cone was allowed to penetrate the female cone at a rate of 2 mm/s keeping a clearance of 2 mm from the base of the female cone. Subsequently, male cone was retracted back to the starting position at the same rate.⁴²

pH Measurement

The pHs of the gels were measured as per the method reported earlier.⁴³ A digital ATC pH meter (EI instruments, model no-132E) was used for the purpose. pH of the topical formulations provide an idea whether the formulation will be irritant to the skin.⁹

Gel–Sol Transition Study

The gel–sol transition temperatures of the gels were determined as per the reported literature.⁴⁴ In short, the gels were incubated in a precision-temperature water-bath whose temperature was varied from 30°C to 50°C. An increment of 5°C was made after every 5 min of incubation at the previous temperature. Samples were analyzed by inverting vials after each incubation period. The temperature at which sample started to flow under gravity was recorded as gel–sol transition temperature (T_g).⁴⁵

Melting Point Determination

The melting point (T_m) of gel samples was determined by the drop-ball method³² using EI melting point apparatus 931 as reported previously.⁴⁶ The gels were taken in 5 mL test-tubes having a diameter of 10 mm. A stainless steel ball (0.1 g, 1.0 mm) was kept on to the surface of the solidified gel. The test-tube was subsequently placed in the sample-holder of the melting-point determination apparatus. The temperature of the sample holder was maintained by using a silicone oil-bath. The heating rate of the sample was 1°C/min. With the increase in the temperature, the structural integrity of the gels was compromised and the ball started to sink. The temperature at which the ball reached the bottom of the tube was taken as the T_m of the gels.

Thermal Analysis. Differential scanning calorimeter (DSC 200F3 Maia, Netzsch, Germany) was used to study the thermal properties of the developed gels. Aluminium pans, whose lids have been pierced, were used for the study. The study was conducted under nitrogen environment. The nitrogen gas was purged at a flow-rate of 40 mL/min. The gels were analyzed in

the temperature range of 30 and 120°C, at a heating-rate of 2°C/min.^{47–49} Effect of incorporation of the drug, MZ, on thermal behavior of the formulations was also studied.

Gel Disintegration Test. The disintegration properties of the gels were studied using the U.S.P. tablet-disintegration apparatus (Electronics, Model 901, Mumbai, India). Accurately weighed ~1.0 g of the gels were molded into tablet shaped (diameter = 1.2 cm, thickness = 0.7 cm) discs. The molded gels were placed in each tube of the disintegration apparatus. Water was used as the disintegrating media. The temperature of the disintegrating media was maintained at $37 \pm 2^\circ\text{C}$. The frequency of the up and down movement of the basket was set at 30 ± 2 cycles/min. The times required by the gel to completely disintegrate, characterized by absence of any gel fraction over the mesh screen of the apparatus, was noted.

Antimicrobial Evaluation. *Bacillus subtilis* (gram positive bacteria) and *Escherichia coli* (gram negative bacteria) were used as model microbes to analyze antimicrobial efficacy of the drug loaded gels. Solid nutrient agar was used as the culture media. About 100 μL of the inoculum (containing 10^{-6} to 10^{-7} cfu/mL) was spread on the solidified agar plates with a sterilized L-shaped spreader. Wells of 5 mm diameter were created with a borer. The wells were filled with the drug loaded gels. Blank gel served as the negative control while powdered drug served as the positive control. The petri-plates were subsequently incubated at 37°C, for 24 h. The zone of inhibition was measured after 24 h of incubation.¹⁶

Hemocompatibility test

The hemocompatibility test was conducted as per the reported method.^{50,51} The test was designed to figure out the extent of hemolysis in the presence of organogel leachants. Accurately weighed 1.0 g of gels was put into the dialysis bags (cellophane membrane, MW cut-off: 60 kDa). The gel-containing dialysis bags were subsequently immersed in 50 mL of saline solution for 30 min. About 0.5 mL of the aliquot was used for the test. Eight milliliters of the citrated goat blood was diluted with 10 mL of normal saline. About 0.5 mL of the diluted blood was taken in a centrifuge tube followed by the addition of the 0.5 mL of the test solution. Final volume was made up to 10 mL by adding normal saline in the centrifuge tube. About 0.5 mL of hydrochloric acid (0.1N) and 0.5 mL of normal saline was used as the positive and negative controls, respectively. The tubes were incubated at 37°C for 1 h and were subsequently centrifuged at 3000 rpm for 10 min. The optical density (OD) of the supernatant was determined at 545 nm using a UV–VIS spectrophotometer (UV 3200 double beam, Labindia). The percentage hemolysis was calculated by the following formula.⁵²

$$\% \text{ Hemolysis} = \frac{\text{OD}_{\text{Test}} - \text{OD}_{\text{Negative}}}{\text{OD}_{\text{Positive}} - \text{OD}_{\text{Negative}}} \times 100 \quad (1)$$

In Vitro Drug Release. *In vitro* release of MZ from the gel formulations were carried out using a two-compartment modified Franz's diffusion cell.⁵³ In short, accurately weighed (~1.0 g) MZ-containing gels was taken in the donor compartment. The receptor compartment contained 50 mL of DW, kept on stirring

Table I. Composition of the Organogel for Determination of CGC

S. No.	Formulations	SMP (% w/w)	CO (% w/w)	Remarks
1	G1	1	99	No gel formation
2	G2	5	95	No gel formation
3	G3	10	90	No gel formation
4	G4	15	85	No gel formation
5	G5	20	80	No gel formation
6	G6	21	79	No gel formation
7	G7	22	78	No gel formation
8	G8	23	77	Gel formation with slight flow
9	G9	24	76	Gel formation with slight flow
10	G10	25	75	Gel formation
11	G11	30	70	Gel formation

at 100 rpm and the temperature was maintained at $37 \pm 1^\circ\text{C}$. Previously activated dialysis membrane (MW cut-off: 60 kDa, Himedia, Mumbai) served as a semi-permeable membrane, which separated the donor compartment from the receptor. At regular intervals (15 min for the first 1 h, 30 min for the next 3 h, and 60 min for the next 8 h) of time, 50 mL of the receptor fluid was completely replaced with fresh 50 mL of DW. The replaced fluid was analyzed using UV-visible spectrophotometer at 321 nm. The drug release kinetics from the gels was studied.

RESULTS AND DISCUSSION

Preparation of Organogel

The dissolution of SMP in CO at 60°C resulted in the formation of a transparent homogenous solution. As the temperature of the hot solution was lowered below 60°C , the gelator (SMP) molecules started to precipitate out of the CO and formed a cloudy suspension of acicular crystals of gelator molecules. This may be accounted to the change in the solubility parameter of the gelator molecules. Upon further standing, the cloudy

suspension formed a gel (if the concentration of the gelator is above the CGC), confirmed by the tube-inversion method (Figure 1 and Table I).

The formation of gel may be attributed to the growth of the acicular crystals into long fibers to form a 3D network structure.⁵⁴ The CGC for the SMP-CO organogels was found to be 25% (w/w). The organogel with 25% of the SMP was regarded as G10.

The physical properties of G10 organogel were modulated by adding various proportions of DW (Figure 2). The proportion of water was varied from 0 % to 100 % (w/w) (Table II). With the increase in the proportions of water, there was a subsequent improvement of the texture of the gels (Supporting Information Figure S1). The apparent viscosity and the consistency of the gels were found to be higher in gels with higher proportions of DW.

Organoleptic Evaluation

G10 gel was yellowish-white in color. The gel was oily and gritty to touch. The gels containing water were milky white in color. There was an increase in the degree of whiteness of the gels as the proportion of water was increased. The gels, GW1, GW2, and GW3, were non-homogenous and gritty in nature whereas the rest of the gels were found to be homogenous and had a smooth texture (Supporting Information Figure S1). The gels were found to be stable after 24 h, when kept at room-temperature (RT, 25°C).

Accelerated Stability Test

The mechanism of destabilization of the gels may be studied under extreme temperature conditions. Any alterations in the physicochemical properties of the components of the gels may result in the destruction of the network structure and may ultimately result in the destabilization of the gels.⁵⁵ The results of accelerated stability test after five freeze-thaw (FT) cycles of the gels have been tabulated in Table II and shown in Supporting Information Figure S2. The results suggested that only GW5 and GW6 gels were stable among the water-containing gels. GW5 was chosen as the representative water-containing organogel for further studies. The resulting gels obtained after the stability test was regarded as G10FT and GW5FT.

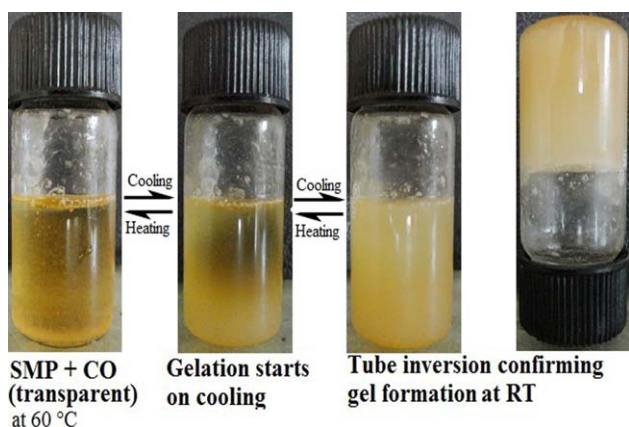


Figure 1. Mechanism of gel formation of CO-SMP organogels. [Color figure can be viewed in the online issue, which is available at wileyonlinelibrary.com.]

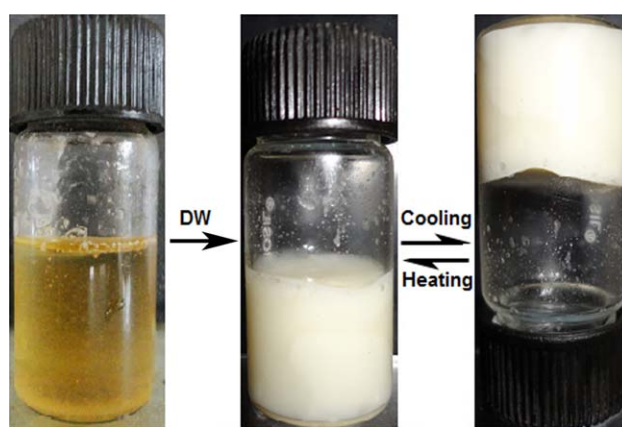


Figure 2. Mechanism of gel formation of water-containing CO-SMP organogels. [Color figure can be viewed in the online issue, which is available at wileyonlinelibrary.com.]

Table II. Composition and Organoleptic Evaluation of CO-SMP Based Organogels

S. No.	Formulations	DW (%w/w of CGC)	DW (%w/w actual)	SMP (%w/w actual)	Observations/comments	
					Freshly prepared gel samples	Gels after accelerated stability test
1	G10	00	00.00	25.00	Homogenous and smooth gel, Slightly yellowish	Homogenous and smooth gel
2	GW1	20	16.66	20.83	Non homogenous and inconsistent gel, no flow	Phase separation and flow on inversion
3	GW2	40	28.50	17.85	Non homogenous and inconsistent gel, no flow	Phase separation and flow on inversion
4	GW3	60	37.50	15.62	Non homogenous and inconsistent gel, no flow	Homogeneity and consistency of the gel was lost, very slight flow
5	GW4	80	44.50	13.88	Homogenous and smooth gel, milky white	Homogeneity and consistency of the gel was lost, very slight flow
6	GW5	90	47.36	13.15	Homogenous and smooth gel, milky white	Homogenous and smooth gel
7	GW6	100	50.00	12.50	Homogenous and smooth gel, milky white	Homogenous and smooth gel

Long-Term Stability Study

The optimized gels were also found to be stable when incubated at $30^{\circ}\text{C} \pm 2^{\circ}\text{C}$ and $75\% \pm 5\%$ RH for 12 months. This suggested that the optimized gels were stable for long periods and hence may be used for developing formulations for commercial use.

Microscopic Studies

The microstructures of the G10 and GW5 gels have been shown in Figure 3(a,b). The micrograph of G10 gel showed small fibers which formed an interconnecting network structure. The

microstructure of GW5 showed uniformly distributed spherical globules throughout the continuous phase [Figure 3(b)].

There was not much difference in the microstructure of the G10 gel after the accelerated stability test. The micrograph suggested that the small fibers were uniformly present throughout the gel matrix [Supporting Information Figure S3(a)]. On the other hand, the internal phase droplets of GW5 gel showed an increase in the sizes of dispersed phase globules with a subsequent decrease in the number of globules with a consequent

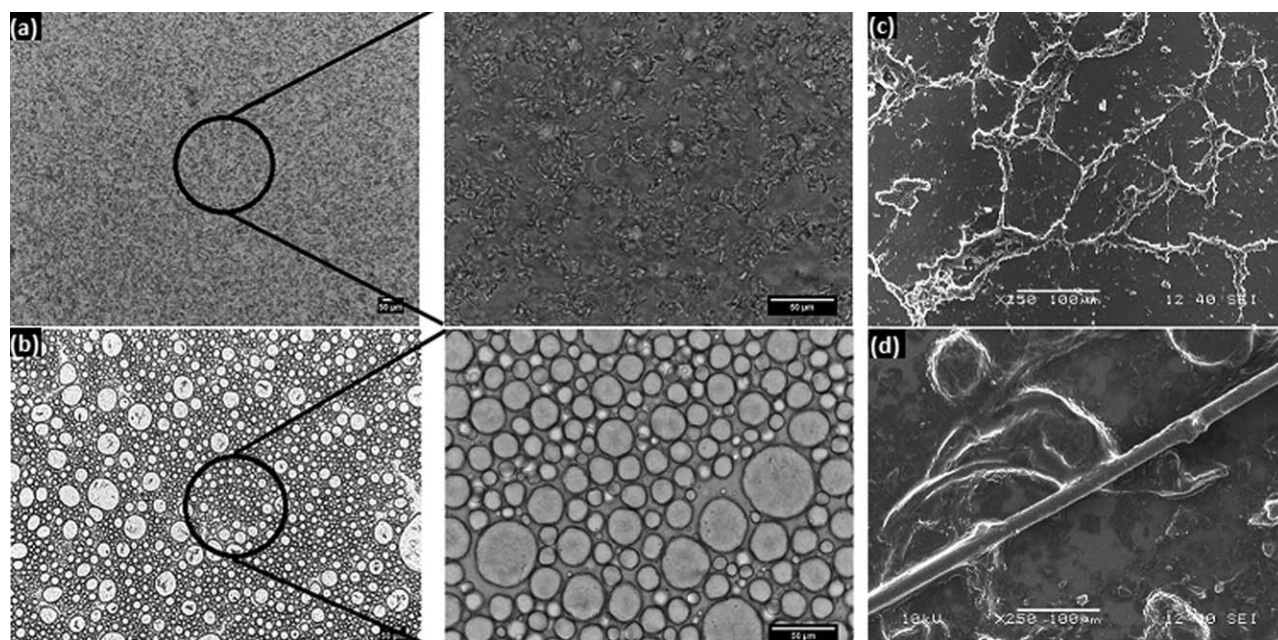


Figure 3. Micrographs obtained under bright field microscopy (a) G10 (b) GW5 and scanning electron microscopy (c) G10 and (d) GW5.

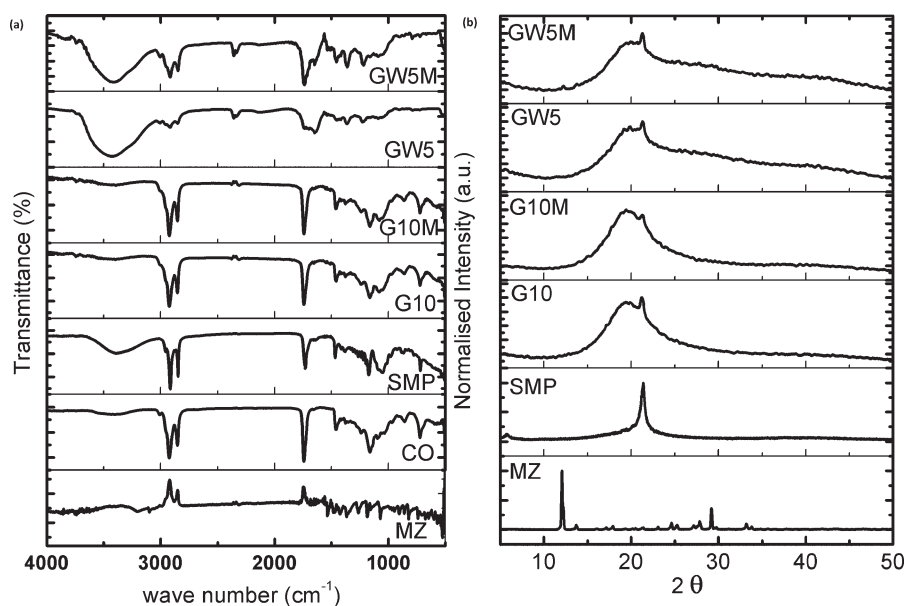


Figure 4. Physico-chemical properties of the optimized gels (a) FTIR Spectra and (b) XRD diffractograms.

increase in the inter-particle distance amongst the droplets after the accelerated stability test. In addition to this, some of the droplets became distorted [Supporting Information Figure S3(b)]. This may be associated with the agglomeration internal droplet phase which may ultimately lead to the separation of the internal phase.⁵⁶ However, since the formulation has been found to withstand five cycles of thermo-cycling, the gel may be expected to be stable for a long period of time.⁵⁷

The sizes of the droplets of the internal phase of the GW5 gel were determined using NI Vision Assistant 2010 image processing software (Supporting Information Figure S4).

The size distribution of the droplets showed an exponential decrease in percent particles. The maximum number of droplets were having a size of $\sim 10 \mu\text{m}$ (33%) followed by droplets of size $\sim 25 \mu\text{m}$ (25%). The cumulative droplet size distribution suggested 50% of the droplets were having droplet size of $\sim 15 \mu\text{m}$. The internal phase droplet size distribution of the GW5FT (GW5 gel after the accelerated stability test) gels was similar to that of the GW5 gel. Most of the droplets were having the droplet size of $\sim 10 \mu\text{m}$ (33%). A small hump in the range of $150\text{--}250 \mu\text{m}$ suggested $<5\%$ of the droplets have undergone coagulation. There was no significant change in the size of the internal phase having 50% of the droplets. The analysis of the micrographs of the GW5 and GW5FT gels suggested that there was no significant change in the droplet size distribution after the accelerated stability testing. This gave an indication that the GW5 gels may be considered as stable gel, though there was an indication of droplet coalescence (Supporting Information Figure S5).^{58,59} Fluorescent microscopic results suggested that the GW5 gel was an organogel and not a hydrogel (Supporting Information Figure S6).

The internal structure of the organogels were analyzed under scanning electron microscope by converting the gels into xerogels (gel devoid of the external continuum phase).⁶⁰ The

micrographs of the xerogels have been shown in Figure 10. The micrographs of G10 gel demonstrated the presence of fiber-like inter-woven network structures. The microstructure of the GW5 gel has shown fiber-like structure in addition to the globular structures. The fibrous structures showed branches of fibers. The branching of the fibrous structures was more in the G10 gel as compared to the GW5 gel. The GW5 gel contained DW within the cores of the vesicular spherical and tubular structures.⁹ Though the results are exciting, there might be some polymorphic transitions during solvent removal or breakage of network junction zones when the xerogels were formed.⁶¹ Also, there are chances of collapse of network onto itself during the extraction of the CO.⁶² These factors might have altered the structural properties of the xerogels and hence the SEM micrographs might not represent the actual structure of the organogels. These results were also supported by the AFM studies (Supporting Information Figure S7).

FTIR Spectroscopy

The FTIR spectroscopy was used to study the molecular interactions amongst the components of the gels. The FTIR spectrograms of the gel components, blank gels, and MZ-loaded gels (G10M and GW5M) have been shown in Figure 4(a). CO showed absorption peaks at $\sim 1730 \text{ cm}^{-1}$ and $\sim 1460 \text{ cm}^{-1}$, which may be associated with the carbonyl group of ester and CH bending vibrations, respectively.⁶³ The absorption peaks at $\sim 2930 \text{ cm}^{-1}$ and $\sim 2837 \text{ cm}^{-1}$ in CO may be attributed to the C–H stretching vibrations in CH_3 and CH_2 due to the alkane backbone of the fatty acids.^{64,65} The absorption peaks at $\sim 1474 \text{ cm}^{-1}$ and $\sim 1373 \text{ cm}^{-1}$ was due to the CH_2 and CH_3 scissoring vibrations.⁶⁶ The peak at $\sim 1743 \text{ cm}^{-1}$ may be associated with the stretching vibration of carbonyl group of the triglycerides present in CO.⁶⁷ SMP showed a broad peak at $\sim 3398 \text{ cm}^{-1}$ which may be due to the presence of intramolecular hydrogen bonding amongst the SMP molecules.⁹ The

Table III. FWHM and AUC Values of the Gels

Formulations	FWHM \pm SD (cm)	Area \pm SD (cm ²)
G10	6.14 \pm 0.15	3019.18 \pm 38
G10M	6.26 \pm 0.21	3345.11 \pm 25
GW5	10.12 \pm 0.22	4933.76 \pm 66
GW5M	11.12 \pm 0.17	5575.17 \pm 46

absorption peaks at $\sim 2930\text{ cm}^{-1}$ and $\sim 2850\text{ cm}^{-1}$ may be associated to the C–H stretch in CH₂ and CH₃ present in the alkanes. An absorption peak at $\sim 3220\text{ cm}^{-1}$ in MZ was due to O–H stretching while the peak at $\sim 3100\text{ cm}^{-1}$ may be associated with C–H stretching. The peak in the range of $1400\text{--}1535\text{ cm}^{-1}$ was due to the imidazole ring.⁶⁸ The peak at 1348 cm^{-1} may be associated with the N=O symmetrical stretching in the imidazole ring. The absorption peak at $\sim 1732\text{ cm}^{-1}$ was due to the presence of C=C double bond.⁶⁹ All

the absorption peaks of the gel components were preserved in the developed organogels. The presence of broad peak at $\sim 3400\text{ cm}^{-1}$ suggested the presence of strong intramolecular/intermolecular hydrogen bonding among the gel components in the blank and MZ-loaded gels. The increase in the intensity of the absorption peaks as compared to the raw materials indicated an increase in the hydrogen bonding amongst the gel components.

XRD Analysis

The XRD diffractograms of the gel components and the gels have been shown in Figure 4(b). Presence of a sharp peak at $21^\circ 2\theta$, corresponding to a Bragg distance (*d*-spacing) of 4.154 \AA , indicated the crystalline nature of SMP. The diffractogram of MZ suggested crystalline nature of MZ due to the presence of a sharp peak at $12^\circ 2\theta$ and low intensity sharp peaks at 24.67° , 27.87° , and $29.30^\circ 2\theta$. The XRD profile of the gels showed a broad peak at $\sim 21.3^\circ 2\theta$ suggested predominantly amorphous nature of the gels. The amorphous nature of the gels may be

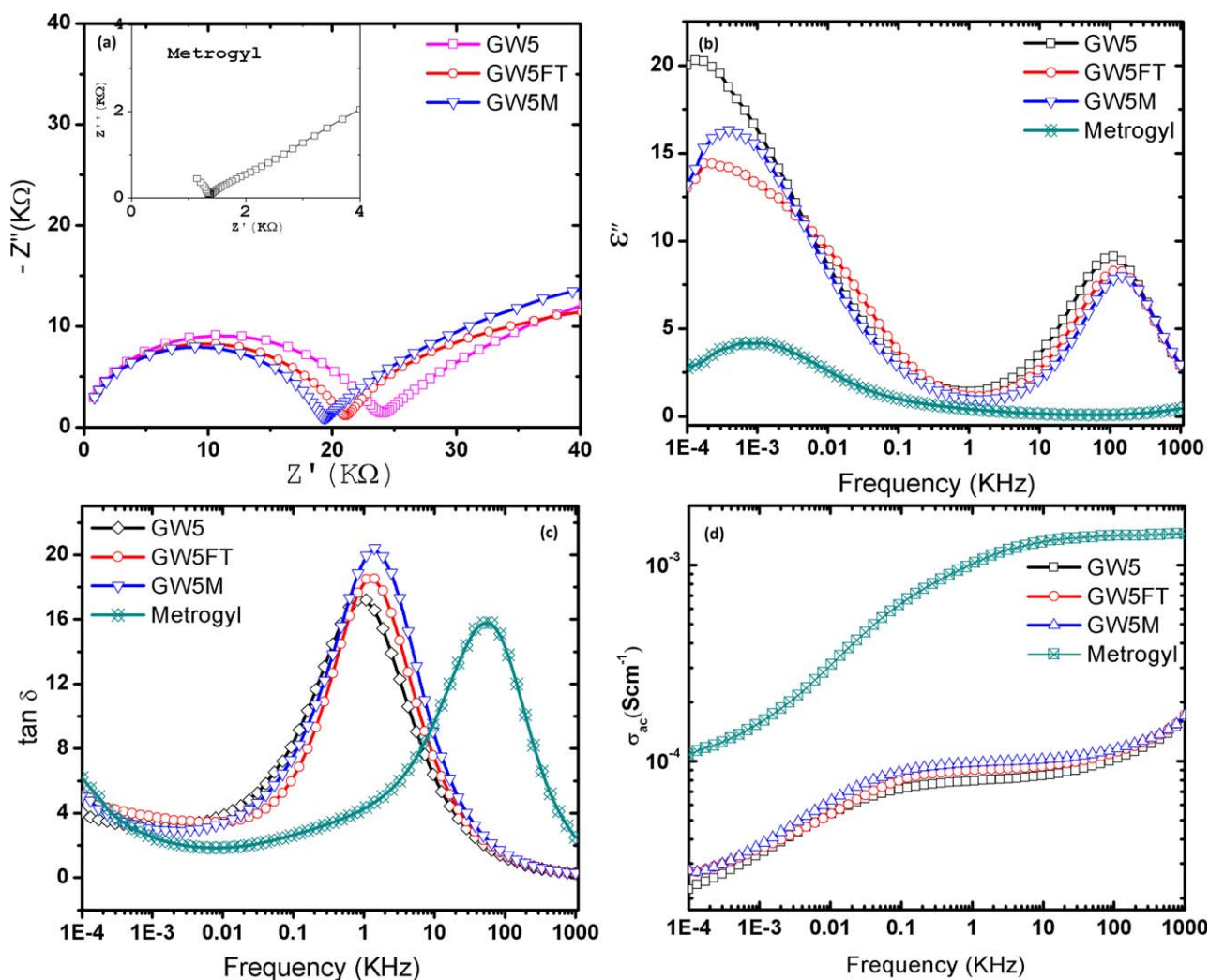


Figure 5. Impedance spectroscopy (a) Nyquist plot of different gel formulations. (b) Variation of imaginary part of permittivity (ϵ'') with frequency for different gel formulations. (c) Frequency dependent dielectric loss ($\tan \delta$) for different gel formulations. (d) Frequency dependent ac conductivity (σ_{ac}) of different gel formulations. [Color figure can be viewed in the online issue, which is available at wileyonlinelibrary.com.]

Table IV. DC Conductivity (σ_{dc}) of Various Gels

Formulations	DC conductivity (σ_{dc}) ($\times 10^{-4}$) (Scm $^{-1}$)
GW5	0.89 \pm 0.02
GW5FT	0.97 \pm 0.05
GW5M	1.07 \pm 0.04
Metrogyl	15.48 \pm 0.26

related to the absence of solid-fibrillar networks.¹⁰ The lower crystalline fraction may be associated with the presence of the inverse micellar structures, evident from the SEM micrographs of the gels.⁷⁰ Absence of any peak corresponding to the MZ explained the complete solubilization of MZ in the apolar phase of the gels.^{71–73} No significant difference was observed in the full width at half maximum (FWHM) and area under the curve (AUC; calculated by the software Fityk) parameters amongst the gels and their drug-containing counterpart (Table III).⁷⁴

Impedance Spectroscopy

Figure 5(a) represents the complex impedance spectrum/Nyquist plot (Z'' vs. Z') of the gels at RT. The absence of water in G10 resulted in very high impedance of the gels. Due to this reason, the gel system acted as an open circuit and no meaningful result was obtained. The complex impedance spectra of GW5 and Metrogyl showed comprises of a broadened semicircle.²³ The results suggested resisto-capacitive equivalent circuit. The intercept of the semicircle on the real axis (Z') gives the bulk resistance (R_b) of the gels.^{37,75} The presence of MZ decreased the diameter of the semi-circle due to an increase in the conductivity of the gels associated with increased amorphosity. The resistive component of the gels was reduced after the accelerated stability test and may be associated with the structural changes within the gels.

The dielectric relaxation provides information about the relaxation response of a dielectric medium to an external electric field of varying frequencies [Figure 5(b)]. The dielectric loss occurs due to the reorientation of the dipoles within the polymer chains and is indicated by dielectric permittivity (ϵ'') spectra.³⁷ The decrease in the ϵ'' in the low frequency region may be attributed to the movement of the charged molecules within the gelled structures while the appearance of peak in higher frequency region have been attributed to the relaxation phenomena of polymer.⁷⁵ The GW5FT did not show any significant difference in the behavior of ϵ'' . Two relaxation peaks were observed in the formulations containing MZ. The relaxation peak in higher frequency region may be associated with the internal structure of the gel. The presence of relaxation peak in the lower frequency region of both Metrogyl[®] and the MZ containing organogels may be associated with the presence of MZ.^{76,77}

There was no significant difference in the $\tan \delta$ of the FT and drug containing gels as compared to the GW5 gel [Figure 5(c)]. Metrogyl showed tangent loss in the higher frequency side. The peak shift in higher frequency region indicated decrease in the relaxation time associated with the faster relaxation of the network structure of the Metrogyl gel. This may be due to its more amorphous nature as compared to the developed gels.⁷⁸

Figure 5(d) shows the variations in the ac conductivity (σ_{ac}) of different formulations with frequency at RT. The low frequency dispersion was observed due to space charge polarization and material electrode interface.³⁷ All the developed formulations showed a near overlapping ac conductivity (σ_{ac}) profile suggesting approximately similar ac conductivity of the gels. The low frequency dispersion was observed due to space charge polarization and material electrode interface.³⁷ There was no significant difference in dc conductivity (Table IV) after FT and incorporation of MZ into the developed gels.⁷⁹ Metrogyl showed very high conductivity due to the presence of water as the continuum phase.⁸⁰

Viscosity Analysis

An exponential decrease in the viscosity of the gels was observed as the shear rate was increased and vice-versa [Figure 6(a)]. This suggested shear-thinning in the gels and indicated a non-Newtonian pseudoplastic flow behavior.⁸¹ This suggests that the stability of the formulations improves when the viscosity is higher at lower shear rates as during storage conditions.⁸² At the same time, a lower viscosity during the application of

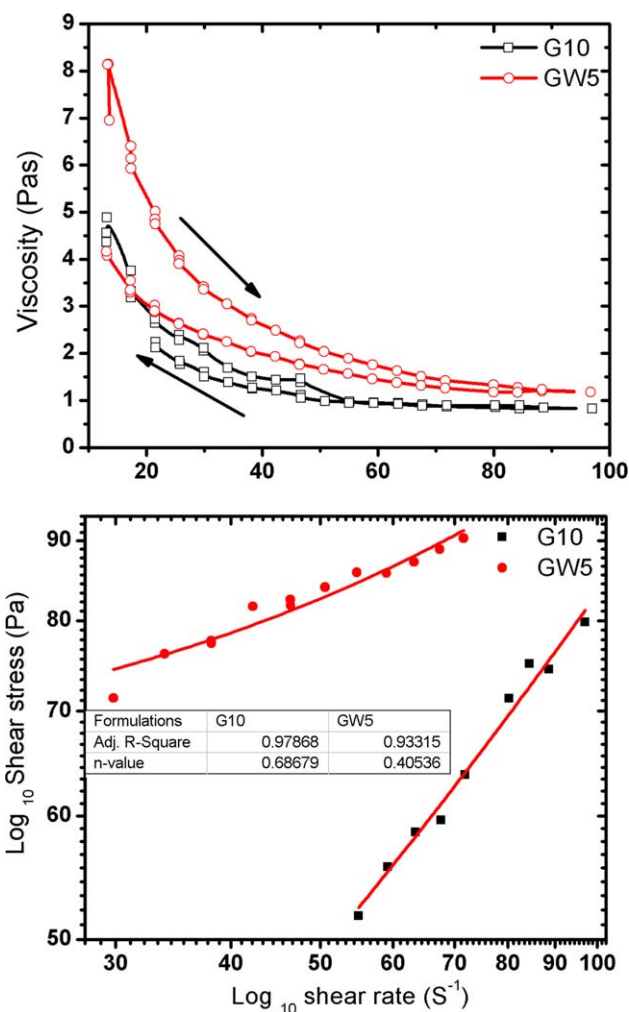


Figure 6. Viscosity profile of the G10 and GW5 gels (a) Shear strain versus Viscosity and (b) $\log \tau$ versus $\log \dot{\gamma}$. [Color figure can be viewed in the online issue, which is available at wileyonlinelibrary.com.]

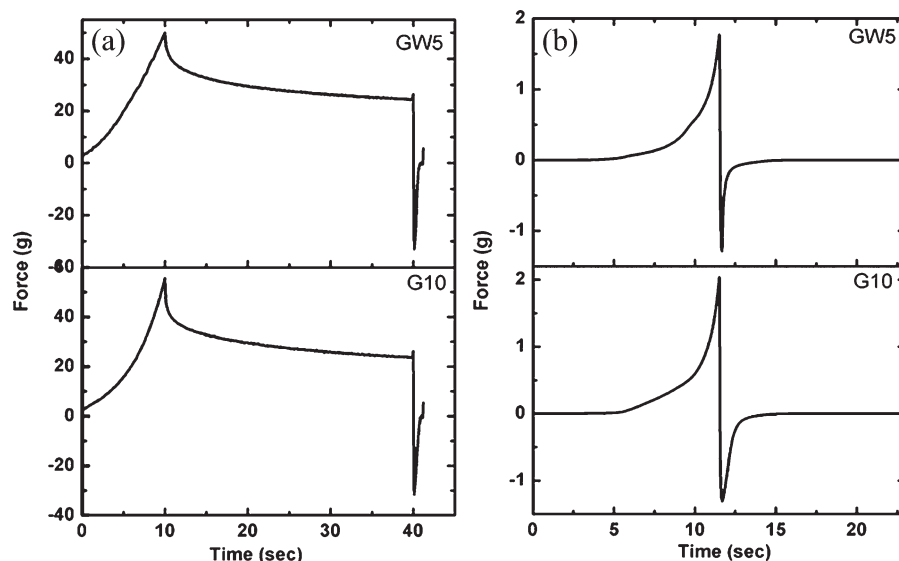


Figure 7. Texture analysis (a) stress relaxation test and (b) spreadability test.

the formulation allows easy application.³⁹ The flow behavior index (n value) was calculated from the Ostwald–de Waele relationship [Figure 6(b)].⁸³ The n values were found to be <1 , suggesting pseudo-plastic behavior of the gels.

Both the gels showed higher apparent viscosities during upward curve of shear rate and comparatively lower apparent viscosities during downward curve. This resulted in the formation of a hysteresis loop.^{84,85} In addition to shear-thinning behavior, the gels showed thixotropic behavior which was attributed to the existence of hysteresis loop in the viscosity profile.^{81,85,86} As observed in hysteresis loop, 100% structure recovery did not take place under the experimental conditions. Such profiles are very common in topical/transdermal drug delivery system.^{87,88}

Texture Analysis

The textural properties of the optimized gels (e.g., stress relaxation and spreadability) were studied (Figure 7, Table V; Supporting Information Table SI and SII).^{41,42,89} The results of the stress relaxation studies suggested that G10 gel was firmer than the GW5 gels. This was evident from the D_{10} values. The percentage relaxation of the G10 was lower than the GW5 gels suggesting that the molecular rearrangement to absorb the energy within the GW5 gel was higher as compared to the G10

gel. This may be associated to the presence of water in GW5 gel.^{90–92}

Similar to the stress relaxation studies spreadability studies also suggested higher firmness of G10 gel. The lower firmness and area of work done for the GW5 gel confirmed higher spreadability of the GW5 gel as compared to G10 gel. The adhesiveness of the G10 gel was higher as compared to the GW5 gel but the stickiness of both the gels was comparable.⁹³

pH Measurement

The pH of the topical/transdermal formulations should lie within the limits of normal skin pH. The pHs of the gels were found to be in the range of 6.5 and 7.0 suggesting the probable non-irritant nature of the gels.⁹⁴ There was no significant change in the pH after drug incorporation (Supporting Information Table SIII).

Gel-to-Sol Transition Study

Gel-to-sol transition temperature (T_{gs}) of the organogels was determined by inverted test-tube method (Table VI). T_{gs} of G10 and GW5 was found to be 40 and 50°C, respectively. This may be attributed to the requirement of more energy for the disruption of the densely packed network structure when water was incorporated within the gels. Incorporation of MZ did not

Table V. Parameters Calculated from Stress Relaxation and Spreadability Studies

Formulations	F_0 (g)	F_{30} (g)	Work done (Relaxation) (g.sec)	% Relaxation	D_{10} (mm)
Stress relaxation studies					
G10	56.395	23.752	859.886	42.118	1.589
GW5	50.423	24.548	865.466	48.684	1.334
Formulations	Firmness (kg)		Cohesiveness (kg s)	Stickiness (kg)	Adhesiveness (kg s)
Spreadability studies					
G10	2.036		2.834	-1.31	-0.139
GW5	1.77		2.447	-1.285	-0.093

Table VI. Gel–Sol Transition Study

Formulations	30°C	35°C	40°C	45°C	50°C
G10	√	√	X	X	X
G10M	√	√	X	X	X
GW5	√	√	√	√	X
GW5M	√	√	√	√	X

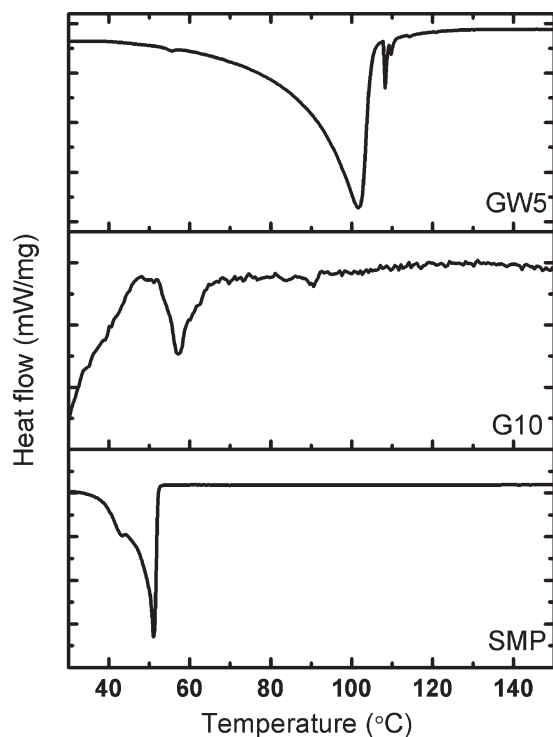
show any significant difference in T_{gs} in both G10 and GW5 gels indicating absence of any interaction between MZ and other components of the blank gel formulations.

Melting Point Determination

The melting point (MP) of the organogels has been tabulated in Supporting Information Table SIV. The MP of G10 was found to be 39.5°C whereas the MP of GW5 was found to be 48.5°C. The results were in accordance with the gel-to-sol transition temperature. The MP of the MZ loaded gels was similar to the corresponding blank gels. The results suggested an increase in the thermal stability of the water containing organogels due to the increase in the intermolecular hydrogen bonding.

Thermal Analysis

The thermal properties of the organogels (G10 and GW5) were studied using a differential scanning calorimeter (Figure 8 and Table VII). An endothermic peak at ~56°C was observed in both the gels. This peak may be associated with the endothermic peak due to the presence of SMP. In addition to the peak at ~56°C, the GW5 gel showed another broad endothermic peak at ~102°C, which may be associated with the evaporation of the aqueous phase at the said temperature. The ΔH_m (change

**Figure 8.** DSC thermograms of SMP, G10, and GW5 gel.**Table VII.** Thermal Properties of Optimized Gels

Formulations	Peak (°C)	ΔH_m (J/g)	ΔS_m (mJ g ⁻¹ K ⁻¹)
SMP	51.1	111.3	436.0792
G10	56.9	2.427	5.932507
GW5	55.6, 101.7	957.1	4475.893

in enthalpy) and ΔS_m (change in entropy) values was calculated for the SMP, G10, and GW5 gels. ΔH_m and ΔS_m was found to be higher in GW5 gel as compared to the G10 gel. This was attributed to the formation of a stable formulation when water was added into the organogel structure. The higher ΔH_m may be associated with the higher intermolecular hydrogen bonding. The results may be correlated with the viscosity analysis, where the viscosity of the GW5 gel was found to be higher as compared to the G10 gel.^{32,49,73}

Gel Disintegration Test

Both the gels disintegrated within a span of 3 min (Supporting Information Table SV). The disintegration time of the GW5 gel was higher as compared to the G10 gel. This is due to the improved stability of the GW5 gels, as has been discussed earlier. This may be explained due to presence of stronger intermolecular hydrogen bonding amongst the water containing gels.⁹⁵

Antimicrobial Test

Both types of the drug loaded organogels showed comparable antimicrobial activity as compared to Metrogyl[®] (Table VIII). The blank gels did not show any antimicrobial property. The study suggests that the developed matrices may be effectively tried for the delivery of antimicrobials.⁹⁶

Hemocompatibility Test

The developed gels (G10 and GW5) showed $\leq 1\%$ hemolysis (Supporting Information Table SVI). This signifies that gels were highly hemocompatible and may be regarded as biocompatible.^{52,73,97}

In Vitro Drug Release

In vitro drug release study helps in predicting the release profile of the drug and the release kinetics. The release profiles of the drug from the gels have been shown in Figure 9. The results indicated that there was 28% and 84% drug release from G10M and GW5M formulations, respectively. On the other hand, Metrogyl[®] showed ~100% drug release within a span of 8 h. The rate of release of MZ was higher in GW5M as compared to G10M. Higher degree of amorphosity of the GW5M as

Table VIII. Antimicrobial Test Against *B. subtilis* and *E. coli*

Formulations	Zone of inhibition \pm SD (cm)	
	<i>B. subtilis</i>	<i>E. coli</i>
Negative control	0.00 \pm 0.00	0.00 \pm 0.00
Positive control - MZ	2.73 \pm 0.46	2.21 \pm 0.12
Metrogyl [®]	2.40 \pm 0.22	1.34 \pm 0.11
G10M	1.22 \pm 0.18	1.15 \pm 0.18
GW5M	2.11 \pm 0.13	1.18 \pm 0.14

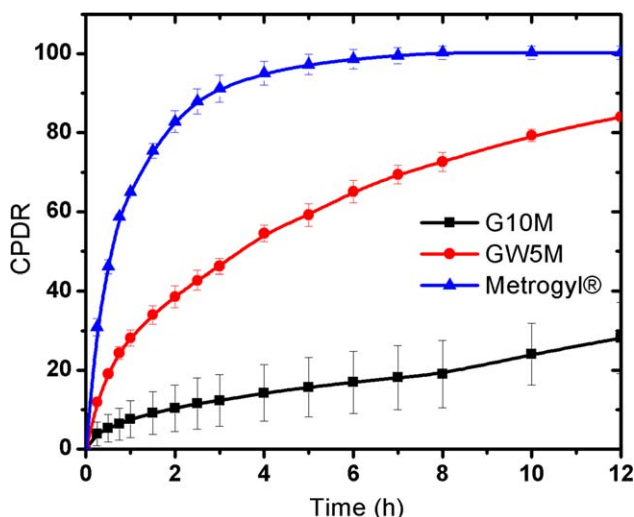


Figure 9. CPDR of the formulations obtained after 12 h of drug delivery. [Color figure can be viewed in the online issue, which is available at wileyonlinelibrary.com.]

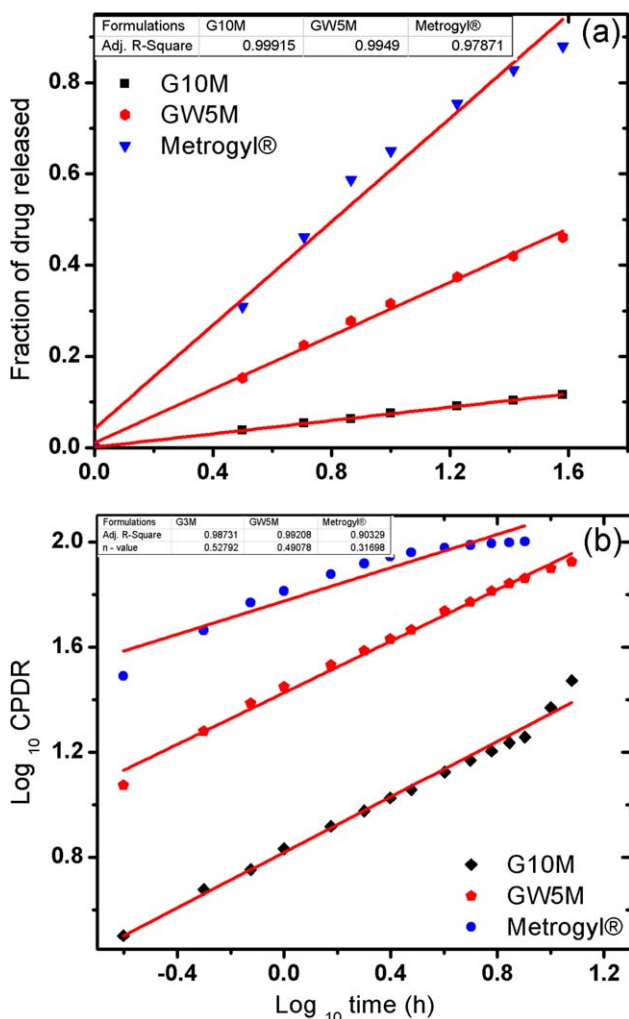


Figure 10. *In vitro* drug release kinetics (a) Higuchi kinetics and (b) K–P model. [Color figure can be viewed in the online issue, which is available at wileyonlinelibrary.com.]

compared to G10M might have promoted the release of the drugs from the matrices. In general, higher the crystallinity of the matrices, slower is the diffusion of the solutes.⁹⁸

The G10M and GW5M formulations followed Higuchian kinetics (Figure 10). The results suggested that the organogels acted as a homogeneous-planar matrix type system.⁹⁹ The “*n*” value calculated from the KP model suggested non-Fickian drug release ($n \approx 0.5$).¹⁰⁰ The release of MZ from Metrogyl® also followed Higuchian release kinetics. The “*n*” value was found to be <0.5 suggesting Fickian diffusion of the drug from the matrices.

CONCLUSION

This study explained the successful development of SMP and CO based organogels as a matrix for controlled drug delivery. The texture of the organogel was found to be smooth and depended on the composition of the gels. The organogels were found to have good spreadability to be used as topical formulations. Apart from this, the gels showed shear thinning and thixotropic behavior which are essential properties of a topical formulation. The organogels were able to modulate the release of the drug from the matrix as the composition of the gels was varied. The preliminary studies suggested biocompatible nature of the gels. The antimicrobial activities of the MZ-loaded gels were found to be similar as compared to the activity of Metrogyl® against the model microorganisms. In gist, the organogels developed in the present study may be used as a carrier for antimicrobial drugs for topical/transdermal applications.

ACKNOWLEDGMENT

The authors acknowledge the financial support received from Department of Biotechnology, New Delhi, India vide sanction order (BT/PR14282/PID/06/598/2010) during the completion of the study.

REFERENCES

- Betageri, G.; Prabhu, S. *Encyclopedia Pharm. Technol.* **2002**, 2, 2436.
- Divani, M. M. J. *IJPRD* **2012**, 4, 104.
- Vintiloiu, A.; Leroux, J. C. J. *Controlled Release* **2008**, 125, 179.
- Almdal, K.; Dyre, J.; Hvidt, S.; Kramer, O. *Polym. Gels Netw.* **1993**, 1, 5.
- Agrawal, V.; Gupta, V.; S. Ramteke, S.; Trivedi, P. *AAPS Pharm. Sci. Technol.* **2010**, 11, 1718.
- Ikeda, S.; Nishinari, K. *J. Agric. Food Chem.* **2001**, 49, 4436.
- Maity, G. C. *J. Phys. Sci.* **2007**, 11, 156.
- Bhattacharya, C.; Kumar, N.; Sagiri, S. S.; Pal, K.; Ray, S. S. *J. Pharm. Bioallied Sci.* **2012**, 4, 155.
- Behera, B.; Sagiri, S. S.; Pal, K.; Srivastava, A. *J. Appl. Polym. Sci.* **2012**, 127, 4910.
- Behera, B.; Patil, V.; Sagiri, S.; Pal, K.; Ray, S. *J. Appl. Polym. Sci.* **2012**, 125, 852.

11. Sagiri, S. S.; Behera, B.; Sudheep, T.; Pal, K. *Designed Monomers Polym.* **2012**, *15*, 253.
12. Imeson, A. *Thickening and Gelling Agents for Food*; Aspen Publishers: New York, **1997**.
13. Murdan, S. *Hospital Pharmacist* **2005**, *12*, 267.
14. Weiss, R. G.; Terech, P. *Molecular Gels: Materials with Self-Assembled Fibrillar Networks*; Kluwer Academic Publisher: Dordrecht, **2006**.
15. George, M.; Weiss, R. G. *Acc. Chem. Res.* **2006**, *39*, 489.
16. Hughes, N. E.; Marangoni, A. G.; Wright, A. J.; Rogers, M. A.; Rush, J. W. E. *Trends Food Sci. Technol.* **2009**, *20*, 470.
17. Bhatia, V.; Barber, R. *J. Am. Pharm. Assoc.* **1955**, *44*, 342.
18. Murdan, S.; Bergh, B.; Gregoriadis, G.; Florence, A. T. *J. Pharm. Sci.* **1999**, *88*, 615.
19. Upadhyay, K. K.; Tiwari, C.; Khopade, A. J.; Bohidar, H. B.; Jain, S. K. *Drug Dev. Ind. Pharm.* **2007**, *33*, 617.
20. Murdan, S.; Gregoriadis, G.; Florence, A. T. *Eur. J. Pharm. Sci.* **1999**, *8*, 177 (1999).
21. Kumar, A.; Sharma, S. *Renew. Sustain. Energy Rev.* **2011**, *15*, 1791.
22. Alvarez, A. M. R.; Rodríguez, M. L. G. *GRASAS Y ACEITES-SEVILLA* **2000**, *51*, 74.
23. Moshkin, V. Castor, AA Balkema, **1986**.
24. Ogunniyi, D. *Bioresour. Technol.* **2006**, *97*, 1086.
25. Scarpa, A.; Guerci, A. *J. Ethnopharmacol.* **1982**, *5*, 117.
26. Tamaru, S.; Uchino, S.; Takeuchi, M.; Ikeda, M.; Hatano, T.; Shinkai, S. *Tetrahedron Lett.* **2002**, *43*, 3751.
27. Hanabusa, K.; Hirata, T.; Inoue, D.; Kimura, M.; Shirai, H. *Colloids Surf. A* **2000**, *169*, 307.
28. Kirilov, P.; Lukyanova, L.; Franceschi-Messant, S.; Perier, V.; Perez, E.; Rico-Lattes, I. *Colloids Surf. A* **2008**, *328*, 1.
29. Yim, Z.; Zupon, M. A.; Chaudry, I. A.. Google Patents, **1989**.
30. Scartazzini, R.; Luisi, P. L. *J. Phys. Chem.* **1988**, *92*, 829.
31. Haering, G.; Luisi, P. L. *J. Phys. Chem.* **1986**, *90*, 5892.
32. Abdallah, D. J.; Weiss, R. G. *Langmuir* **2000**, *16*, 352.
33. Murdan, S.; Gregoriadis, G.; Florence, A. T. *J. Pharm. Sci.* **1999**, *88*, 608.
34. Belgamwar, V.; Pandey, M.; Chauk, D.; Surana, S. *Asian J. Pharm.* **2008**, *2*, 134.
35. Langford, J.; Louër, D.; Scardi, P. *J. Appl. Crystallogr.* **2000**, *33*, 964.
36. Kumar, R.; Katare, O. P. *AAPS Pharm. Sci. Technol.* **2005**, *6*, 298.
37. Pradhan, D. K.; Choudhary, R.; Samantaray, B. *Express Polym. Lett.* **2008**, *2*, 630.
38. Rout, S.; Hussian, A.; Lee, J.; Kim, I.; Woo, S. *J. Alloys Comp.* **2009**, *477*, 706.
39. Neves, J.; Da Silva, M. V.; Gonçalves, M. P.; Amaral, M. H.; Bahia, M. F. *Curr. Drug Deliv.* **2009**, *6*, 83.
40. Krokida, M.; Maroulis, Z. *Drying Technol.* **1999**, *17*, 449.
41. Jena, R.; Bhattacharya, S. *J. Texture Stud.* **2007**, *34*, 349.
42. Bobe, G.; Hammond, E.; Freeman, A.; Lindberg, G.; Beitz, D. *J. Dairy Sci.* **2003**, *86*, 3122.
43. Li, X. Y.; Kong, X. Y.; Wang, X. H.; Shi, S.; Guo, G.; Luo, F.; Zhao, X.; Wei, Y. Q.; Qian, Z. Y. *Eur. J. Pharm. Biopharm.* **2010**, *75*, 388.
44. Shaikh, I. M.; Jadhav, S.; Jadhav, K.; Kadam, V.; Pisal, S. *Curr. Drug Deliv.* **2009**, *6*, 1.
45. Wakerly, Z.; Fell, J.; Attwood, D.; Parkins, D. *J. Pharm. Pharmacol.* **1997**, *49*, 622.
46. van der Laan, S.; Feringa, B. L.; Kellogg, R. M.; van Esch, J. *Langmuir* **2002**, *18*, 7136.
47. Dassanayake, L. S. K.; Kodali, D. R.; Ueno, S.; Sato, K. *J. Am. Oil Chem. Soc.* **2009**, *86*, 1163.
48. Brinksma, J.; Feringa, B. L.; Kellogg, R. M.; Vreeker, R.; van Esch, J. *Langmuir* **2000**, *16*, 9249.
49. Luisi, P.; Scartazzini, R.; Haering, G.; Schurtenberger, P. *Colloid Polym. Sci.* **1990**, *268*, 356.
50. Pal, K.; Pal, S. *Mater. Manuf. Process.* **2006**, *21*, 325.
51. Sutar, P. B.; Mishra, R. K.; Pal, K.; Banthia, A. K. *J. Mater. Sci. Mater. Med.* **2008**, *19*, 2247.
52. Pal, K.; Banthia, A.; Majumdar, D. *J. Mater. Sci. Mater. Med.* **2007**, *18*, 1889.
53. Willimann, H.; Walde, P.; Luisi, P.; Gazzaniga, A.; Stroppolo, F. *J. Pharm. Sci.* **1992**, *81*, 871.
54. Trivedi, D. R.; Ballabh, A.; Dastidar, P.; Ganguly, B. *Chem. A Eur. J.* **2004**, *10*, 5311.
55. Rabinow, B. E. *Nat. Rev. Drug Discov.* **2004**, *3*, 785.
56. Kawashima, Y.; Cui, F.; Takeuchi, H.; Niwa, T.; Hino, T.; Kiuchi, K. *Int. J. Pharm.* **1995**, *119*, 139.
57. Gooch, J. W. *Emulsification and Polymerization of Alkyd Resins*; Springer: New York, **2002**.
58. Han, J.; Davis, S. S.; Washington, C. *Int. J. Pharm.* **2001**, *215*, 207.
59. Kalaria, D.; Sharma, G.; Beniwal, V.; Ravi Kumar, M. N. V. *Pharm. Res.* **2009**, *26*, 492.
60. Markovic, N.; Dutta, N. K. *Thermochim. Acta* **2005**, *427*, 207.
61. Tamura, T.; Suetake, T.; Ohkubo, T.; Ohbu, K. *J. Am. Oil Chem. Soc.* **1994**, *71*, 857.
62. Rogers, M. A.; Smith, A. K.; Wright, A. J.; Marangoni, A. G. *J. Am. Oil Chem. Soc.* **2007**, *84*, 899.
63. Luo, X.; Xiao, W.; Li, Z.; Wang, Q.; Zhong, J. *J. Colloid Interface Sci.* **2009**, *329*, 372.
64. Muik, B.; Lendl, B.; Molina-Diaz, A.; Valcarcel, M.; Ayora-Cañada, M. J. *Anal. Chim. Acta* **2007**, *593*, 54.
65. Ifuku, S.; Tsujii, Y.; Kamitakahara, H.; Takano, T.; Nakat-subo, F. *J. Polym. Sci. Part A Polym. Chem.* **2005**, *43*, 5023.
66. Atek, D.; Belhaneche-Bensemra, N. *Eur. Polym. J.* **2005**, *41*, 707.
67. Pérez-Mateos, M.; Montero, P.; Gómez-Guillén, M. C. *Food Hydrocolloids* **2009**, *23*, 53.
68. Yuan, J.; Liu, M. *J. Am. Chem. Soc.* **2003**, *125*, 5051.

69. Cristescu, R.; Popescu, C.; Popescu, A.; Grigorescu, S.; Mihailescu, I.; Mihaiescu, D.; Gittard, S.; Narayan, R.; Buruiana, T.; Stamatina, I. *Appl. Surf. Sci.* **2009**, *255*, 9873.
70. Luo, X.; Li, Z.; Xiao, W.; Wang, Q.; Zhong, J. *J. Colloid Interface Sci.* **2009**, *336*, 803.
71. Yu, H.; Xiao, C. *Carbohydr. Polym.* **2008**, *72*, 479.
72. Bot, A.; Veldhuizen, Y. S. J.; den Adel, R.; Roijers, E. C. *Food Hydrocolloids* **2009**, *23*, 1184.
73. Roy, S.; Pal, K.; Thakur, G.; Prabhakar, B. *Mater. Manuf. Process.* **2010**, *25*, 1477.
74. Azároff, L. V.; Kaplow, R.; Kato, N.; Weiss, R. J.; Wilson, A.; Young, R. X-ray Diffraction; McGraw-Hill: New York, **1974**.
75. Ramesh, S.; Wong, K. *Ionics* **2009**, *15*, 249.
76. He, R.; Craig, D. Q. M. *J. Pharm. Sci.* **1999**, *88*, 635.
77. Bonacucina, G.; Palmieri, G. F.; Craig, D. Q. M. *J. Pharm. Sci.* **2005**, *94*, 2452.
78. Hanabusa, K.; Hiratsuka, K.; Kimura, M.; Shirai, H. *Chem. Mater.* **1999**, *11*, 649.
79. Pissis, P.; Kyritsis, A. *Solid State Ionics* **1997**, *97*, 105.
80. Pradhan, D. K.; Samantaray, B.; Choudhary, R. N. P.; Thakur, A. K. *Ionics* **2005**, *11*, 95.
81. Zhu, C.; Smay, J. E. *J. Rheol.* **2011**, *55*, 655.
82. Yang, Y.; Wang, S.; Xu, H.; Sun, C.; Li, X.; Zheng, J. *Asian J. Pharm. Sci.* **2008**, *3*, 175.
83. Jones, D. S.; Muldoon, B. C. O.; Woolfson, A. D.; Andrews, G. P.; Sanderson, F. D. *Biomacromolecules* **2008**, *9*, 624.
84. Chhatbar, M. U.; Prasad, K.; Chejara, D. R.; Siddhanta, A. *Soft Matter* **2012**, *8*, 1837.
85. Desai, H.; Biswal, N. R.; Paria, S. *Ind. Eng. Chem. Res.* **2010**, *49*, 5400.
86. Jibry, N.; Heenan, R. K.; Murdan, S. *Pharm. Res.* **2004**, *21*, 1852.
87. Korhonen, M.; Hellen, L.; Hirvonen, J.; Yliruusi, J. *Int. J. Pharm.* **2001**, *221*, 187.
88. Jones, D. S.; Brown, A. F.; Woolfson, A. D. *J. Pharm. Sci.* **2001**, *90*, 1978.
89. Mao, R.; Tang, J.; Swanson, B. *J. Food Sci.* **2008**, *65*, 374.
90. Rohm, H.; Weidinger, K. H. *J. Texture Stud.* **1993**, *24*, 157.
91. Hatcher, D.; Bellido, G.; Dexter, J.; Anderson, M.; Fu, B. *J. Texture Stud.* **2008**, *39*, 695.
92. Turgeon, S. L.; Beaulieu, M. *Food Hydrocolloids* **2001**, *15*, 583.
93. Kealy, T. *Food Res. Int.* **2006**, *39*, 265.
94. Kamble, S.; Udapurkar, P.; Biyani, K.; Nakhat, P.; Yeole, P. *Inventi Rapid: NDDS*, **2011**.
95. Kawasaki, N.; Ohkura, R.; Miyazaki, S.; Uno, Y.; Sugimoto, S.; Attwood, D. *Int. J. Pharm.* **1999**, *181*, 227.
96. Figueiredo de Almeida Gomes, B. P.; Vianna, M. E.; Sena, N. T.; Zaia, A. A.; Ferraz, C. C. R.; de Souza Filho, F. J. *Oral Surg. Oral Med. Oral Pathol. Oral Radiol. Endodontol.* **2006**, *102*, 544.
97. Pal, K.; Bag, S.; Pal, S. *Trends Biomater. Artif. Organs* **2005**, *19*, 39.
98. Frank, A.; Rath, S. K.; Venkatraman, S. S. *J. Controlled Release* **2005**, *102*, 333.
99. Varshosaz, J.; Tabbakhian, M.; Salmani, Z. *Open Drug Deliv. J.* **2008**, *2*, 61.
100. Sawant, P. D.; Luu, D.; Ye, R.; Buchta, R. *Int. J. Pharm.* **2010**, *396*, 45.